Atomic force microscopy study of surface topography of films of cholesteric oligomer- and polymer-based mixtures with photovariable helix pitch

Alexey Bobrovsky,* Olga Sinitsyna, Sergei Abramchuk, Igor Yaminsky, and Valery Shibaev
Faculty of Chemistry, Moscow State University, Lenin Hills, Moscow, 119991 Russia
(Received 14 September 2012; published 18 January 2013)

The surface topography of glass-forming polymers and oligomer cholesteric systems with a phototunable helix pitch was studied. For this purpose several mixtures based on nematic polyacrylate and cholesteric cyclosiloxanes doped with chiral-photochromic dopant were prepared and investigated. The molecules of chiral-photochromic dopant consist of isosorbide chiral moiety and cinnamic C=C double bonds capable of E-Z photoisomerizing. UV irradiation of the planarly oriented films of mixtures leads to dopant photoisomerization and changes of its helical twisting power. During this process irreversible changes of helix pitch values take place, which allows one to obtain the same cholesteric systems with different helix pitch values. The films of the annealed mixtures were studied by atomic force microscopy and transmission electron microscopy. The correlations between the features of surface topography and helix pitch of cholesteric supramolecular structure were found and discussed.

DOI: 10.1103/PhysRevE.87.012503 PACS number(s): 61.30.Vx

I. INTRODUCTION

The study of interfacial phenomena, surface topography, and interactions between different phases attracts a great deal of attention. In particular, it is a very interesting and important topic in the field of liquid crystalline self-organized systems [1–6].

One of the great advantages of polymer materials is the unique possibility to "freeze" bulk and surface structure in a rigid glassy state that is convenient for research using different types of microscopy techniques including atomic force microscopy (AFM) [7–9]. A competition between bulk and surface free energies results in the appearance of surface deformation and defects in nematic, smectic, and cholesteric liquid crystals [7–11]. In particular, cholesteric mesophases show very unusual topography at the free surface which is determined by a competition between the homeotropic boundary condition at the interface between the air and the liquid crystal and the planar orientation in the bulk of the films [7,8]. Focal conic domains appear as micron-sized "hills" having a double-spiral superstructure.

As was shown by Mitov and co-workers, surface topography and defects in cholesteric materials containing nanoparticles can be successfully used for the nanoparticles' ordering [12–14]. These studies demonstrated that the nanoparticles' patterns depend strongly on the film thickness. The authors also observed the influence of the nanoparticles' presence and concentration on the optical properties (selective light reflection) of the composites.

On the other hand, the introduction of the photochromic moieties in polymer systems capable of photochemical transformations allows one to create materials with photocontrollable structure and optical properties [15–19]. There is a huge number of papers devoted to the investigation of the so-called photoinduced surface relief grating phenomena in azobenzene-containing polymer and low-molar-mass materials [19–25]. Molecular motion over distances much larger than the molecule size is photoinduced upon irradiation within the absorption band of the chromophores, which induces the formation of surface relief gratings.

Photochromic liquid crystal (LC) systems forming a cholesteric phase due to the combination of unique optical properties of cholesteric mesophases with the ability to be photocontrolled are of special interest.

It is well known that the cholesteric mesophase is characterized by the helical supramolecular organization of mesogens, which determines its unique optical properties [26]. One of these optical properties is the selective reflection of light with wavelength λ_{max} depending on helix pitch (P) of the cholesteric structure according to the equation

$$\lambda_{max} = \langle n \rangle P, \tag{1}$$

where $\langle n \rangle$ is the average refractive index of liquid crystal.

The specific value of the selective reflection wavelength depends on many internal and external factors. One of these factors is the structure and geometry of the chiral fragments responsible for the helical twisting of the whole system. The key parameter characterizing the ability of chiral groups for twisting cholesteric mesophases is the helical twisting power, expressed by the simple equation

$$\beta = dP^{-1}/dX = \langle n \rangle \left(d\lambda_{max}^{-1}/dX\right)_{X=0}, \tag{2}$$

where X is the concentration of the chiral fragments.

A number of interesting approaches for photoregulation of selective light reflection wavelength were developed [27–41]. One of them is based on the introduction of combined chiral-photochromic fragments capable of photoisomerization into a cholesteric or nematic matrix. Under the irradiation the helical twisting power of the chiral-photochromic dopant decreases leading to the reversible or irreversible shift of selective light reflection wavelength.

As mentioned above, the synthesis of cholesteric polymers and preparation of the polymer-based mixtures allow one to create glass-forming materials with optical properties "frozen" in the glassy state for a prolonged time [28,34–41]. This advantage is very significant for the creation of new materials for optical data recording and storage.

*bbrvsky@yahoo.com

In this connection it seems to be very important to establish a definite correlation between the helix untwisting in such polymer materials and the peculiarities of their surface relief topography. In particular, it would be essential to study the influence of UV light irradiation on the helix pitch as well as on the period of double-spiral structure on the film's surface, which was found earlier in nonphotochromic systems [7–9].

In this work we have prepared cholesteric mixtures based on nematogenic polymer PAA and oligomeric cholesteric cyclosiloxanes (SilBlue, SilRed):

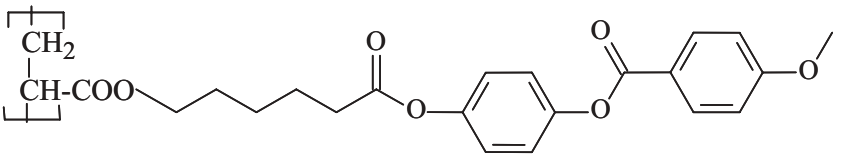

PAA

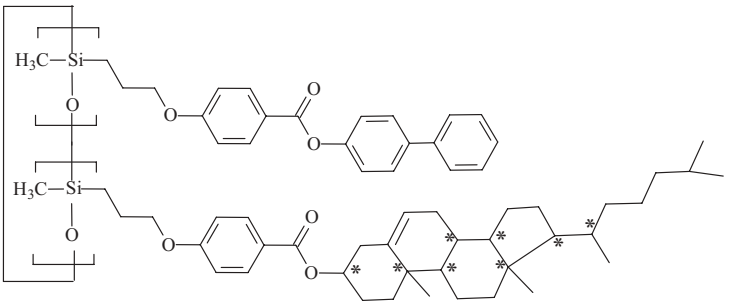

SilBlue, SilRed

Polymer PAA forms a nematic phase with clearing temperature 135 °C and glass transition $T_g \sim 30$ °C.

Cyclosiloxanes SilBlue, SilRed form a left-handed cholesteric mesophase with a wide temperature range (clearing temperatures are above 180 °C, $T_g \sim 50$ °C) and contain different concentrations of biphenyl and chiral cholesterol-containing monomer units determining different helix pitch values and selective light reflection wavelength: in blue ($\lambda_{max} \sim 450$ nm) for SilBlue or red ($\lambda_{max} \sim 650$ nm) for SilRed spectral regions. Relatively high T_g of such materials makes them very convenient for atomic force microscopy (AFM) measurements.

A cinnamoyl derivative of isosorbide (Sorb) was used as a chiral-photochromic dopant.

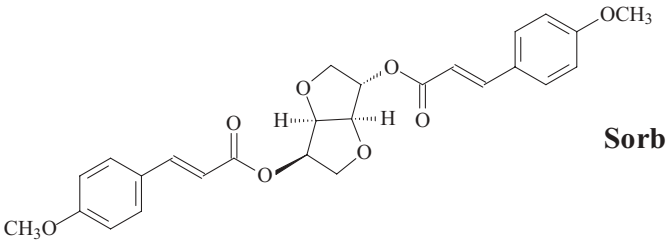

Sorb

This right-handed chiral compound has a high twisting ability (35–40 μm^{-1}, depending on the matrix) and can undergo *E-Z* isomerization leading to decreasing its helical twisting power due to the reduction of the molecular anisometry (Fig. 1) [42,43]. Introducing a chiral dopant into the nematic phase of PAA induces right-handed helix formation. On the other hand, the introduction of right-handed dopant into the left-handed cholesteric cyclosiloxanes results in partial "compensation of chirality," and therefore partial helix untwisting takes place. Thus, UV irradiation of planarly oriented films of PAA-based mixture leads to helix untwisting, whereas for mixtures based on SilRed and SilBlue the helix pitch decreases. Isomerization and helix twisting (untwisting) processes are thermally completely irreversible (up to temperatures of thermal degradation, above 200 °C). This fact makes the dopant Sorb very convenient for fine phototuning of the cholesteric helix pitch values by changing the time of UV irradiation, which was followed by sample annealing and the fixation of obtained cholesteric structure in a glassy state at room temperature.

Taking all this into account, we have prepared several mixtures based on polymer and oligomer matrices containing different concentrations of Sorb. The main goal of the paper is to study the influence of photoirradiation on the cholesteric systems, paying special attention to the investigation of the peculiarities and regularities of the changing surface morphologies of these samples depending on photoregulated helix pitch values.

II. EXPERIMENT

A. Materials

Nematic polymer PAA and chiral-photochromic dopant Sorb were synthesized according to previous papers [42,44]. Cholesteric cyclosiloxanes were used as received from Wacker Chemie.

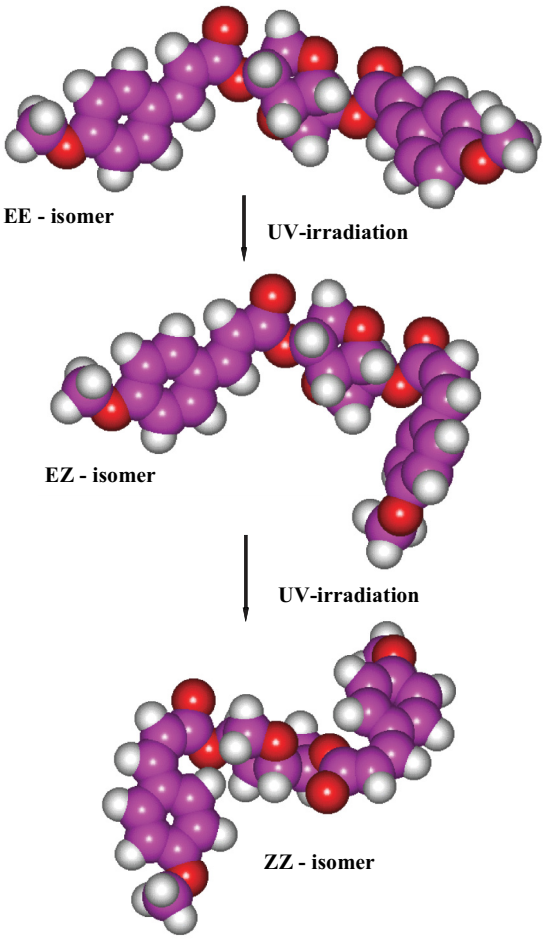

FIG. 1. (Color online) *E-Z* isomerization process taking place under UV irradiation of chiral photochromic dopant Sorb.

A sample of PAA was obtained by fractionation [44] and has a degree of polymerization of 87 and polydispersity of 1.15 as determined by gel permeation chromatography using a Knauer instrument, with the solvent being THF.

1. Characterization of phase behavior and optical properties

The phase transition temperatures of the polymer fractions and mixtures were studied by differential scanning calorimetry (DSC) with a PerkinElmer DSC-7 thermal analyzer with a scanning rate of 10 K/min.

The polarizing microscope investigations were performed using a Mettler TA-400 thermal analyzer and a LOMO P-112 polarizing microscope. Selective light reflection (transmittance) spectra were studied using Hitachi U3400 UV-Vis-NIR and Unicam UV-500 UV-Vis spectrophotometers. The values of the cholesteric pitch were calculated using the maximum wavelength of the selective light reflection in Eq. (1), $P = \lambda_{\max}/\langle n \rangle$, assuming the average refractive index for such type of mesogenic materials to be about 1.6.

B. Sample preparation

Cholesteric mixtures were prepared by dissolving compounds in chloroform (a good solvent for all matrices and dopant) followed by slow evaporation at room temperature and drying in vacuum at ~100 °C for 1 h.

Samples for the photo-optical and AFM investigations were prepared as follows. Small amounts (a few milligrams) of the mixture were heated up to 110 °C (mixtures based on PAA) or 140 °C (mixtures based on cyclosiloxanes) on a glass substrate and covered by another glass plate. For planar orientation of cholesteric mesophase the top glass was uniaxially shifted several times with respect to the bottom one with the rate of about 5–10 mm/s and amplitude ~3–5 mm. Then samples were annealed at the same temperature. After that, cells were disassembled by accurately shifting glass plates in order to obtain the free film surface for AFM. Next the films were annealed (10 min per sample), and then cooled down to room temperature at two different rates, very fast (a couple of minutes) or slowly (1°/min). The thickness of the cholesteric films was more than 10 μm.

C. Photo-optical investigations

For the cholesteric helix pitch phototuning we have used a special instrument equipped with a DRSh-350 ultrahigh pressure mercury lamp and UV light-emitting diode (LED) (emission maximum 365 nm). For the lamp light, a wavelength of 365 nm was selected using interference filters. To prevent heating of the samples due to IR irradiation of the lamp, a water filter was used. The intensity of light was equal to ~2.0 mW/cm^2, (lamp) and ~0.5 mW/cm^2 (LED) as measured by a LaserMate-Q (Coherent) intensity meter. Spectral measurements were performed using a photodiode array UV-visible spectrometer (J&M Analytik). Before studying the helix untwisting kinetics, the samples were irradiated by UV light during different time periods at room temperature. After that, samples were annealed at 110 °C (mixtures based on PAA) or 140 °C (mixtures based on cyclosiloxanes); the shift of selective light reflection peak was monitored by the spectrometers.

D. AFM and transmission electron microscopy study

The surface structure of the samples was investigated by AFM in the tapping mode. The measurements were performed using a scanning probe microscope (FemtoScan) in air at room temperature. We used cantilevers produced by Mikromasch with a typical resonant frequency of 325 kHz and a typical probe tip radius of 10 nm. Processing and image analysis were performed with the software FEMTOSCAN ONLINE [45]. Since the surface of the samples simultaneously contained elements with different heights, large-scale elements were subtracted in the case of the analysis of elements with low height. For this purpose an image was divided into 1024 squares. In each square, the average height was calculated and assigned to the central point. A bicubic spline was constructed for the surface using these points and then subtracted from the surface.

Thin cut films of the samples (80–100 nm) were prepared using an ultramicrotome (Reichert-Gung) with a diamond knife (Diatome) and different cutting rates (from 0.1 to 100 mm/s). For the investigations of structural change across the cutting plane, cuts were performed under a 2° angle with respect to the free surface of the sample, allowing one to observe areas from top to bottom of the sample (almost "in

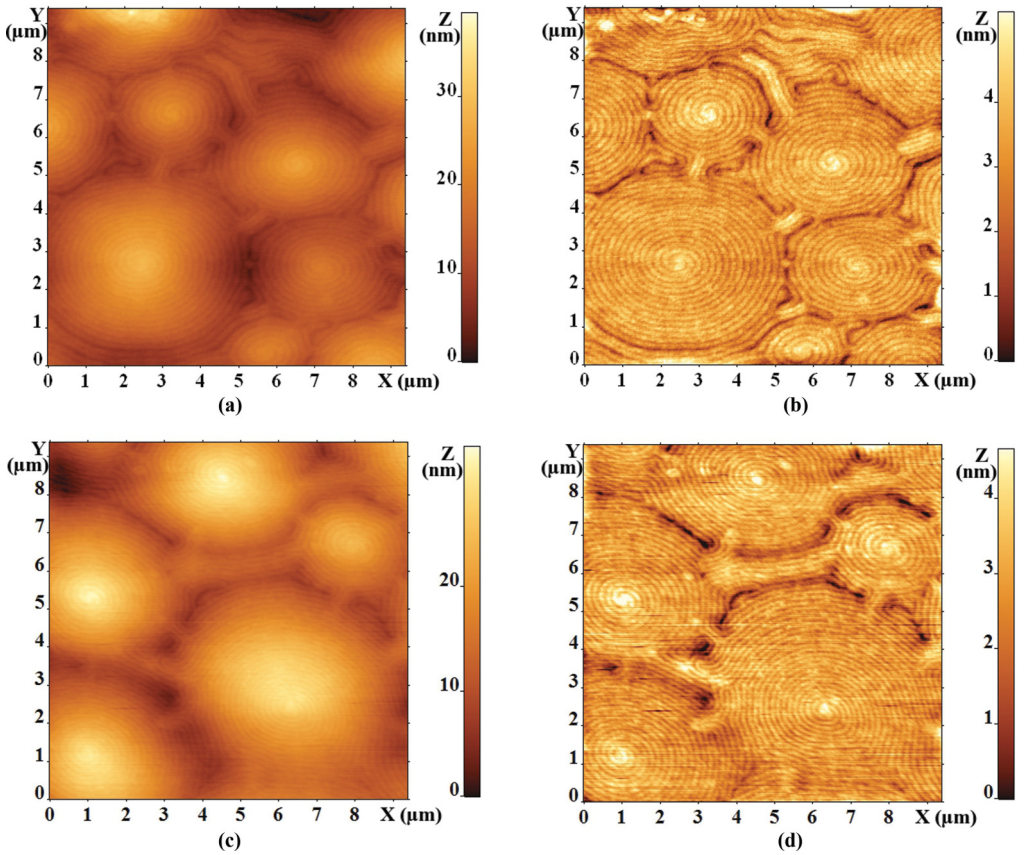

FIG. 2. (Color online) AFM images of mixture SilBlue + Sorb 2% films before (a), (b) and after UV irradiation (c), (d) during 300 s. In (b), (d), large-scale elements were subtracted as described in Sec. II.

plane"). For the structural study of the samples in the plane, orthogonal to the film surface, a series of consecutive cuts (up to 50) in the transverse direction was performed (with the rate of 2 mm/s). Obtained cuts were studied using a transmission electron microscope (LEO 912 AB, Omega Karl Zeiss) with an accelerating voltage of 100 kV.

III. RESULTS AND DISCUSSION

Figures 2(a), 2(b) and 3(a), 3(b) show the AFM images of focal conic domains for cholesteric mixtures SilBlue + Sorb and PAA + Sorb at the free surface, respectively. It should be noticed that due to the thermal prehistory of these films, namely an annealing well above the glass transition temperature and slow cooling down to room temperature, we can be quite sure that all films have more or less an equilibrium mesophase structure. In the bulk of the film near the glass plate the planar orientation of mesogenic groups is realized due to the shifting of substrates before annealing. As seen from Figs. 2 and 3 for both mixtures, the AFM images reveal the cone shape of the focal conic domains with the double-spiral patterns of surface relief at the cholesteric-air interface.

For the mixture SilBlue + Sorb in different parts of the samples, all double spirals have the same sense of rotation

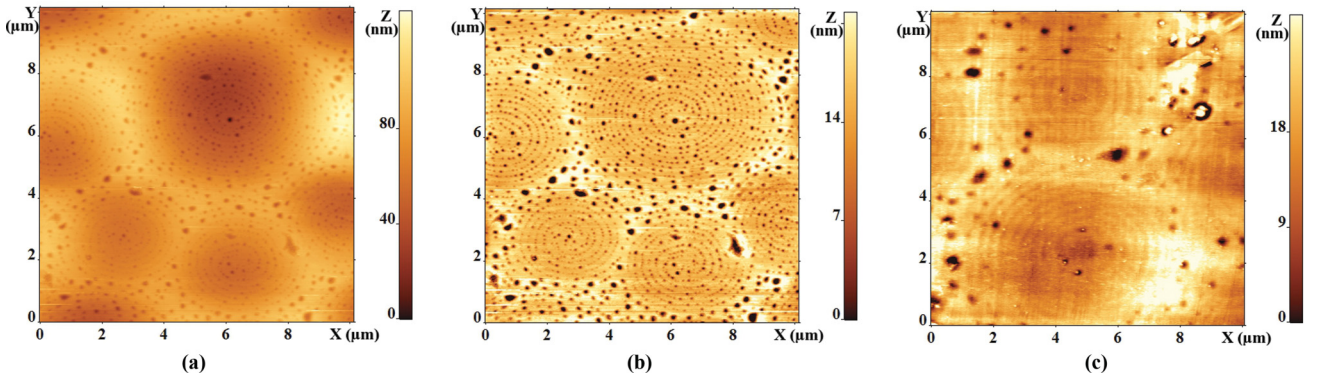

FIG. 3. (Color online) AFM images of mixture PAA + Sorb 5% films before (a), (b) and after UV irradiation (c) during 40 s. In (b), large-scale elements were subtracted.

and possess a conical form with the center at the highest position. The spirals spin clockwise (if viewed starting from the center of each spiral). Such structures are formed due to the competition between the planar orientation of mesogenic groups in the bulk of the films and the tendency of aligning the mesogens homeotropically (normally to the surface) at the cholesteric-air interface [7,8,46] in our open oligomer films with hybrid anchoring. The average height of the cones (the average height difference between the center of the domain and its boundaries with the neighboring domains) is 17 nm. The average diameter is 3.4 μm.

Mixtures of SilBlue + Sorb double spirals form hills, as was observed for the cyclosiloxanes of similar structure before [7,8,46], but it is completely unexpected and unusual that the mixture PAA + Sorb forms "valleys" [Fig. 3(b)]. The average depth of the valleys is 115 nm, and the average diameter is 5.5 μm. For this mixture all observed double spirals also have the same anticlockwise sense of rotation, which is opposite to SilBlue + Sorb films due to the right-handed helical structure of PAA + Sorb mixtures. All spirals possess a conical form with the center at the lowest position. The origin of such extreme difference between SilBlue- and PAA-based mixtures is still unclear but probably it is associated with different values of the elastic constants for cyclosiloxane- and polyacrylate-based LC matrices. The surface of the mixture PAA + Sorb contains a large number of pores with depth from 1 to 100 nm (the average depth is 8 nm). The depth of the pores is considerably less than their diameter, which ranges from 65 to 400 nm (the average pore diameter is 138 nm). Large pores are concentrated in the space between the focal conic domains, while the small pores decorate the double spirals. The origin of these surface features is still unknown.

UV irradiation leads to a change of the cholesteric pitch and shift of the selective light reflection to longer wavelength ranges for the mixture PAA + Sorb (Fig. 4), or to shorter wavelengths for mixtures based on cyclosiloxanes (see also the values of selective light reflection maximum λ_{max} in Table I). Table I summarizes the values of selective light reflection and corresponding helix pitch obtained by spectroscopy as well as the surface relief period as measured by AFM.

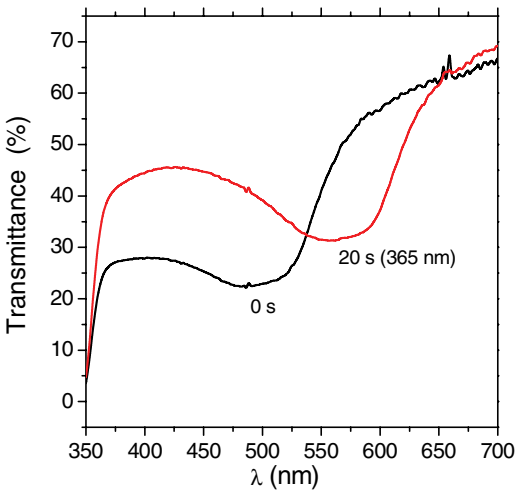

FIG. 4. (Color online) Transmittance spectra of mixture PAA + Sorb 5% before and after UV irradiation.

Photocontrolling of the cholesteric pitch for mixtures based on SilBlue just changes the surface relief period (decreasing it under UV irradiation and annealing) without changing the morphology (Figs. 2 and 3). Short irradiation time (5 s) for the mixture PAA + Sorb leads to the ordering of the small pores within the double spirals. However, long irradiation time (>40 s) diminishes the surface relief, while all topography features become invisible. The depth of the cones decreases to 10 nm. Both mixtures described above have relatively small cholesteric helix pitches (260–430 nm),

TABLE I. Comparison of average surface relief period with selective light reflection wavelength and helix pitch.

Mixture	Irradiation time (s) (thermal prehistory)	λ_{max} (nm)	Pitch (nm)	Sample size N (number of periods)	Average surface period d (nm)	Standard deviations (nm)	Angle α (deg)[a]
PAA + Sorb 5%	0	420	260	75	159	27	55
	5	450	280	100	190	50	47
	20	580	360	96	298	76	37
	40	690	430	47	352	79	38
SilBlue + Sorb 2%	0	480	300	100	167	24	64
	300	438	270	100	140	21	75
SilRed + Sorb 3%	0 Fast cooling	1180	740	80	811	175	27
	0 Slow cooling	1085	680	100	728	189	28
	60 Fast cooling	670	420	100	314	66	42
	60 Slow cooling	690	430	100	357	69	37
	600 Fast cooling	550	~400	100	335	52	37
	600 Slow cooling	600	~400	100	297	52	42

[a]The angles are calculated by Eq. (3).

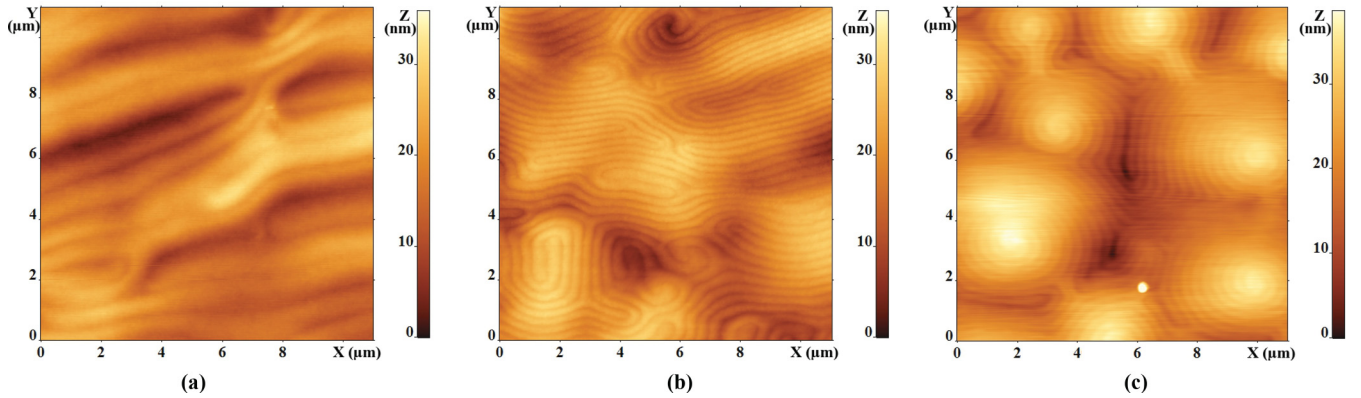

FIG. 5. (Color online) AFM scan of mixture SilRed + Sorb before (a), after 60 s (b), and after 600 s (c) of UV irradiation. The cooling rate was fast.

which correspond to the selective light reflection in the visible spectral range and form double-spiral surface structure with hills for cyclosiloxane-based mixtures and valleys for polyacrylate-based mixtures.

A completely different type of surface topography was found for the cholesteric mixture SilRed + Sorb which has a larger cholesteric pitch in the range of 700 nm (Table I). Before irradiation, the "fingerprint" structure with periodic elongated surface relief is formed [Fig. 5(a)]. At first glance, such patterns remind us of the fingerprint polarizing optical microscopy textures of cholesteric mesophase with large helix pitch (in the micrometer order) [47]. But in analogy with fingerprint textures, the period of the surface structure observed [Fig. 5(d)] should coincide with the half of the cholesteric pitch obtained by the spectrophotometry method. Nevertheless, these values are completely different. For example, for the fast cooled sample with $P/2 = 370$ nm, the measured surface period is more than two times larger, equal to 811 nm (Table I).

As seen clearly in Figs. 5(a)–5(c), the surface topography for the mixture SilRed + Sorb is changed from the elongated fingerprint pattern to the circular double-spiral features with decreasing of the helix pitch induced by UV irradiation. A decrease of the helix pitch to 420–430 nm results in the formation of the intermediate state between fingerprint and circular double-spiral patterns [Fig. 5(b)]; further UV irradiation restores the double-spiral surface structure, which is typical for the cholesteric materials with a helix pitch less than ~400 nm [Fig. 5(c)]. The average diameter of the double spirals is 4.5 μm. Their average height is 19 nm in the case of rapid cooling and 10 nm in the case of slow cooling. The situation is similar to the mixture SilRed + Sorb after irradiation for 60 s. The average heights of the intermediate state are 16 and 6 nm for fast and slow cooling, respectively. Smoother surface is observed in the case of slow cooling.

It is interesting to compare the half of the helix pitch and the period of surface structure of the investigated samples. According to Table I and Fig. 6, the average surface period linearly increases with the half of the helix pitch. The period of the surface structures is almost constant within a double helix, but may vary for different helices, as well as for the regions between them. The standard deviations of the surface periods for different samples are summarized in Table I. The observed surface topography is associated with the

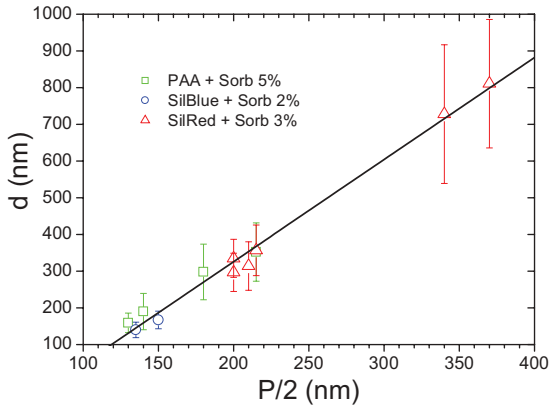

FIG. 6. (Color online) Dependence of surface relief period on pitch of cholesteric helix for all systems. Bars show dispersion of surface period values as calculated from AFM images.

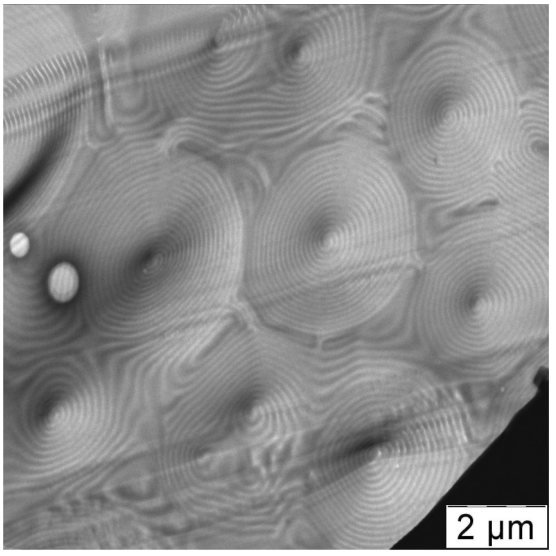

FIG. 7. TEM image of a cut of left-handed cholesteric. The cut is made at an angle of 2° to the free surface of the cholesteric. The sample thickness is about 10 μm. The distance from the free surface is about 2 μm. The cut thickness is about 80 nm.

periodic change in the orientation of the mesogens in the cholesteric phase [7]. Ideal cholesteric liquid crystal can be considered as a system of parallel planes or "layers" of a nematic phase. The mesogen direction is constant in each layer. In the bulk of cholesteric films near the glass substrate the layers are parallel to the surface due to the planar boundary conditions of this interface. The layers incline near the cholesteric-air interface due to the homeotropic boundary conditions. As shown before for cyclosiloxanes, nested-arc structures are formed near the air-sample interface [14]. The smaller the angle of the layers inclination, the larger the period of the surface structure.

In order to clarify the internal structure of the sample, microtome cuts of one of the cholesteric films (SilBlue + Sorb 2% after irradiation in the glassy state) were studied by transmission electron microscopy. The thickness of the resulting cut depends on the orientation of the director due to the local anisotropy of mechanical properties of the sample associated with the local orientation of the mesogens. The largest cut thickness corresponds to the local director orientation in the plane of cutting. This leads to a different image contrast in the electron microscope and allows one to see the "footprints" of the glassy cholesteric director field, because electron irradiation results in the disorientation of mesogens up to the isotropic state [46].

Figure 7 shows the image of a cut made at an angle of 2° with respect to the surface of the cholesteric film. The distance between the cut and the free surface is about 2 μm. The image contains double helices just as in the AFM images of the film surface. Figure 8(a) shows the TEM image of a cut, made

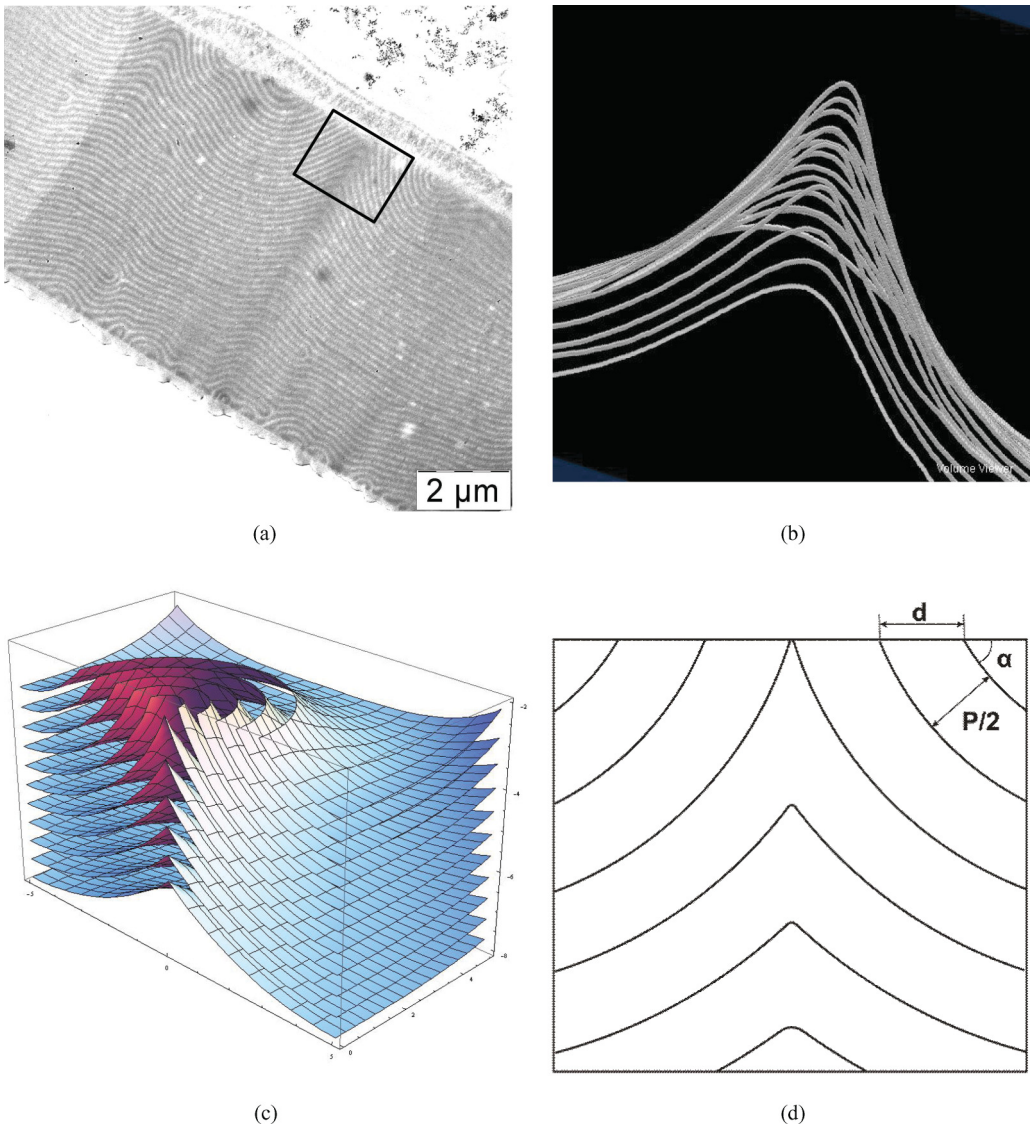

FIG. 8. (Color online) (a) TEM image of cross section of SilBlue + Sorb film. (b) Three-dimensional reconstruction of one of the surfaces near a polygon center for left-handed cholesteric obtained by processing of the electron-microscope images of a series of cuts that are orthogonal to the free surface of the sample. The cuts' thickness (the distance between adjacent curves) is 80 nm. Image size is 2.80 × 2.80 μm. (c) Three-dimensional image of the layers in the form of nested toroidal surfaces [47] in the region of the double helix. (d) Schematical representation of cross section passing through the center of the double-helix core shown by black rectangle in (a). The lines show the perturbation of the cholesteric structure near the surface. At the surface cholesteric layers incline by an angle α relative to the sample plane.

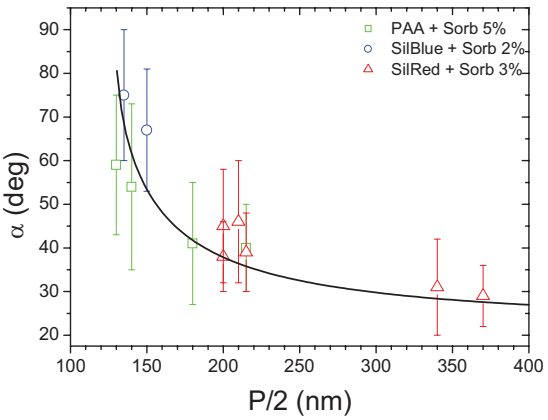

FIG. 9. (Color online) Dependence of the angle of cholesteric layers inclination α on the half of the pitch of the cholesteric helix for all systems. Bars show dispersion of angle α values as calculated from AFM images.

perpendicular to the surface and passing through the center of the double helix. Nested-arc structures are observed near the sample surface. The shape of a layer in the center of the cholesteric double helix was rebuilt using of a series of cuts [Fig. 8(b)]. It is clearly seen that the Gaussian curvature of the layer is negative. The scheme of the three-dimensional arrangement of layers is shown in Figs. 8(c) and 8(d). Nested arcs of cholesteric textures have already been observed by TEM in the cross sections of cholesteric liquid crystal oligomers [8,46], but the model used in [8] cannot be applied to the nested-arc patterns that we observed near the free surface of our samples. In our case, the tops of the conical surfaces are oriented in the direction of the sample's free surface and not the other way, as assumed in the model. On the other hand, the three-dimensional representation of the cholesteric structure proposed in paper [46] is consistent with our results. However, there is no detailed consideration about the origin of the double-helical structures there. Therefore, we have modified the model proposed earlier [8], and explained our experimental results and the nature of the double helix. Calculations revealed that the solution for the director field on the cholesteric film surface is a double spiral of Archimedes for the given configuration of layers, in agreement with the experimental data (see Supplemental Material [48]). It is interesting to note that the main features of the internal structure of the cholesteric annealed in the glassy state with one free surface are in agreement with the internal structure of the polygonal texture in cholesteric liquid crystal (MBBA and Canada balsam), which was studied by optical methods in a series of papers by Bouligand (see, e.g., [49]). Bouligand explained the origin of double spirals in chiral liquid crystals around polygon centers by means of cholesteric layers arranged as nested toroidal surfaces [46] as shown in Figs. 8(c) and 8(d). The difference is that in our case the toroidal surfaces are not orthogonal to the cholesteric-air boundary, making the angle α much less than 90° [Fig. 8(d)].

According to the TEM observations, the inclination angle of layers near the surface is about 70°. Table I contains calculated angles (α) for different samples. The values of the period of surface structures (d) were measured by AFM. It is noteworthy that the slope of the surface is small enough. It does not exceed 5° for PAA + Sorb, and 1° for mixtures based on cyclosiloxanes, so the surface can be considered flat in our approximate calculation:

$$d = p/2 \sin(\alpha). \tag{3}$$

The average inclination angle of the layers near the surface of the cholesteric (SilBlue + Sorb 2% after irradiation) is 75°. Thus, the data obtained by two different microscopic methods are in good agreement.

Figure 9 demonstrates the dependence of α on the half of the pitch of the cholesteric helix for all investigated mixtures. It should be noted that for the larger pitch of the cholesteric helix, the angle of rotation of the cholesteric helix axis at the air-sample interface is smaller. In the case of identical values of cholesteric helix pitch, the angle of the cholesteric helix axis inclination is larger by about 20° for the mixture SilBlue + Sorb than for the mixture PAA + Sorb.

In conclusion, we have investigated the surface topography for the glass-forming polymer and oligomer cholesteric systems with phototunable helix pitch. On the basis of experimental studies, the explanation of the origin of the double helix on the surface of glassy cholesteric films was suggested. It is found that double-helix formation is associated with the curvature of the "cholesteric layers" in a system of nested toroids. Cholesteric layers are tilted with respect to the free surface at constant angle α. Correlations between the features of the surface topography and helix pitch of cholesteric supramolecular structure were found and discussed. Dependence of the surface period on cholesteric helix pitch was determined for systems with a wide variation of helix pitch values. It is shown that the average surface period almost linearly increases with the helix pitch value. For cholesteric mixtures with a large cholesteric pitch (~700 nm) the fingerprint structure instead of double-spiral domains is formed.

ACKNOWLEDGMENTS

This research was supported by the Russian Foundation of Fundamental Research (Grants No. 11-03-01046a, No. 12-03-00553-a, and No. 11-03-12054-OFI-M). The authors thank Dr. N. Boiko for the polyacrylate PAA synthesis.

[1] Th. Rasing and L. Musevic, *Surfaces and Interfaces of Liquid Crystals* (Springer-Verlag, Berlin, Heidelberg, 2004).
[2] Y. Bai and N. L. Abbott, Langmuir **27**, 5719 (2011).
[3] P. Chiarelli, S. Faetti, and L. Fronzoni, J. Phys. **44**, 1061 (1983).
[4] K. Kocevar, R. Blinc, and I. Musevic, Phys. Rev. E **62**, R3055 (2000).
[5] Y. G. J. Lau, S. Klein, C. J. P. Newton, and R. M. Richardson, Liq. Cryst. **34**, 421 (2007).
[6] T. Lopez-Leon and A. Fernandez-Nieves, Colloid Polym. Sci. **289**, 345 (2011).
[7] R. Meister, H. Dumoulin, M.-A. Halle, and P. Pieranski, J. Phys. II **6**, 827 (1996).

[8] R. Meister, H. Dumoulin, M.-A. Halle, and P. Pieranski, Phys. Rev. E **54**, 3771 (1996).
[9] A. Boudet, M. Mitov, C. Bourgerette, T. Ondarcuhu, and R. Coratger, Ultramicroscopy **88**, 219 (2001).
[10] B. D. Terris, R. J. Twieg, C. Nguyen, G. Sigaud, and H. T. Nguyen, Europhys. Lett. **19**, 85 (1992).
[11] D. K. Yoon, M. C. Choi, Y. H. Kim, M. W. Kim, O. D. Lavrentovitch, and H.-T. Jung, Nat. Mater. **6**, 866 (2007).
[12] M. Mitov, C. Portret, C. Bourgerette, E. Snoeck, and M. Verelst, Nat. Mater. **1**, 229 (2002).
[13] M. Mitov, C. Bourgerette, and F. de Guerville, J. Phys.: Condens. Matter **16**, S1981 (2004).
[14] R. Bitar, G. Agez, and M. Mitov, Soft Matter **7**, 8198 (2011).
[15] V. Shibaev, A. Bobrovsky, and N. Boiko, Prog. Polym. Sci. **28**, 729 (2003).
[16] Y. Zhao, Pure Appl. Chem. **76**, 1499 (2004).
[17] V. P. Shibaev, Polym. Sci., Ser. A **51**, 1131 (2009).
[18] V. G. Chigrinov, V. M. Kozenkov, and H.-S. Kwok, *Photoalignment of Liquid Crystalline Materials*, Wiley-SID Series in Display Technology (John Wiley & Sons, New York, 2008).
[19] *Smart Light-Responsive Materials: Azobenzene-Containing Polymers and Liquid Crystals*, edited by Y. Zhao and T. Ikeda (John Wiley & Sons, New York, 2009).
[20] L. M. Goldenberg, Y. Gritsai, and J. Stumpe, J. Opt. **13**, 075601 (2011).
[21] L. M. Goldenberg, L. Kulikovsky, O. Kulikovska, J. Tomczyk, and J. Stumpe, Langmuir **26**, 2214 (2010).
[22] F. Fabbri, D. Garrot, K. Lahlil, J. P. Boilot, Y. Lassailly, and J. Peretti, J. Phys. Chem. B **115**, 1363 (2011).
[23] T. Ikawa, Y. Kato, T. Yamada, M. Shiozawa, M. Narita, M. Mouri, F. Hoshino, O. Watanabe, M. Tawata, and H. Shimoyama, Langmuir **26**, 12673 (2010).
[24] J. Vapaavuori, A. Priimagi, and M. Kaivola, J. Mater. Chem. **20**, 5260 (2010).
[25] A. Ambrosio, A. Camposeo, A. Carella, F. Borbone, D. Pisignano, A. Roviello, and P. Maddalena, J. Appl. Phys. **107**, 083110 (2010).
[26] V. A. Belyakov, *Diffraction Optics of Complex-Structured Periodic Media* (Springer, Berlin, 1992).
[27] B. L. Feringa, R. A. van Delden, N. Koumura, and E. M. Geertsema, Chem. Rev. **100**, 1789 (2000).
[28] A. Bobrovsky, N. Boiko, and V. Shibaev, Liq. Cryst. **24**, 489 (1998).
[29] F. H. Kreuzer, in *Polymers as Electrooptical and Photooptical Active Media*, edited by V. Shibaev (Springer-Verlag, Berlin, Heidelberg, 1996).
[30] C. Ruslim and K. Ichimura, J. Phys. Chem. B **104**, 6529 (2000).
[31] A. I. Krivoshey, N. I. Shkolnikova, N. S. Pivnenko, and L. A. Kutulya, Mol. Cryst. Liq. Cryst. **449**, 21 (2006).
[32] R. van Delden, M. B. van Gelder, N. P. M. Huck, and B. L. Feringa, Adv. Funct. Mater. **13**, 319 (2003).
[33] N. Tamaoki, Adv. Mater. **13**, 1135 (2001).
[34] N. Boiko, L. Kutulia, Yu. Reznikov, T. Sergan, and V. Shibaev, Mol. Cryst. Liq. Cryst. **251**, 311 (1994).
[35] A. Bobrovsky, N. Boiko, and V. Shibaev, Chem. Mater. **13**, 1998 (2001).
[36] M. Brehmer, J. Lub, and P. van de Witte, Adv. Mater. **10**, 1438 (1999).
[37] P. van de Witte, J. C. Galan, and J. Lub, Liq. Cryst. **24**, 819 (1998).
[38] A. Bobrovsky, N. Boiko, and V. Shibaev, Liq. Cryst. **25**, 679 (1998).
[39] A. Bobrovsky, N. Boiko, and V. Shibaev, Liq. Cryst. **26**, 1749 (1999).
[40] P. van de Witte, E. E. Neuteboom, M. Brehmer, and J. Lub, J. Appl. Phys. **85**, 7517 (1999).
[41] A. Bobrovsky, N. Boiko, V. Shibaev, and J. Springer, Liq. Cryst. **28**, 919 (2001).
[42] A. Bobrovsky, N. Boiko, and V. Shibaev, Mol. Cryst. Liq. Cryst. **363**, 35 (2001).
[43] A. Bobrovsky, N. Boiko, V. Shibaev, I. Zavarzin, M. Kalik, and M. Krayushkin, Polym. Adv. Technol. **13**, 595 (2002).
[44] N. Boiko, V. Shibaev, and M. Kozlovsky, J. Polym. Sci., Part B: Polym. Phys. **43**, 2352 (2005).
[45] http://www.femtoscanonline.com/
[46] G. Agez, R. Bitar, and M. Mitov, Soft Matter **7**, 2841 (2011).
[47] P. Oswald and P. Pieranski, *Nematic and Cholesteric Liquid Crystals* (Taylor & Francis Group, Boca Raton, FL, 2005).
[48] See Supplemental Material at http://link.aps.org/supplemental/10.1103/PhysRevE.87.012503 for the mathematical description of the double-spiral structure.
[49] Y. Bouligand, J. Phys. France **33**, 715 (1972).